

Percolation in random sequential adsorption of polydisperse mixtures of extended objects on a triangular lattice

D Dujak¹, A Karač², Z M Jakšić³, S B Vrhovac^{3,*}
and Lj Budinski-Petković⁴

¹ Faculty of Electrical Engineering, University of Sarajevo, Sarajevo 71000, Bosnia and Herzegovina

² Polytechnic Faculty, University of Zenica, Zenica, Bosnia and Herzegovina

³ Institute of Physics Belgrade, University of Belgrade, Pregrevica 118, Zemun 11080 Belgrade, Serbia

⁴ Faculty of Engineering, University of Novi Sad, Trg D. Obradovića 6, Novi Sad 21000, Serbia

E-mail: vrhovac@ipb.ac.rs

Received 26 June 2023

Accepted for publication 30 July 2023

Published 22 August 2023

Online at stacks.iop.org/JSTAT/2023/083209
<https://doi.org/10.1088/1742-5468/accefb>



CrossMark

Abstract. Percolation properties of an adsorbed polydisperse mixture of extended objects on a triangular lattice are studied by Monte Carlo simulations. The depositing objects of various shapes are formed by self-avoiding walks on the lattice. We study polydisperse mixtures in which the size ℓ of the shape making the mixture increases gradually with the number of components. This study examines the influence of the shape of the primary object defining a polydisperse mixture on its percolation and jamming properties. The dependence of the jamming density and percolation threshold on the number of components n making the mixture is analyzed. Determining the contribution of the individual components in the lattice covering allowed a better insight into the deposit structure of the n -component mixture at the percolation threshold. In addition, we studied mixtures of objects of various shapes but the same size.

Keywords: percolation, triangular lattice, object shape, polydisperse mixtures

* Author to whom any correspondence should be addressed.

Contents

1. Introduction	2
2. Definition of the model and the simulation method	3
3. Results and discussion	5
4. Concluding remarks	17
Acknowledgments	18
References	18

1. Introduction

Percolation is a simple model of the formation of long-range connectivity in random systems. In 1957 Broadbent and Hammersley, published the first paper on percolation theory to model the flow of fluid in a random medium [1]. Later on, others applied and generalized the theory, in particular by developing percolation theory on lattices and studying it by computer simulations [2–6]. Percolation has a wide variety of applications, including porous media [7], microemulsions [8], disordered semiconductors and superconductors [9], molecular and macromolecular liquids [10, 11], nano-tubes in composites and suspensions [12, 13], thin metal films [14], layered materials [15], biological networks and bioinformatics [16, 17], etc.

For most real percolating systems, some important physical properties depend on the detailed geometry of the substrate and on the shape and size of the adsorbed particles. Consequently, more general percolation problems can be formulated by including irreversible random deposition of extended objects occupying more than one site on the lattice [18–23]. In random sequential adsorption (RSA) processes particles are randomly, sequentially and irreversibly deposited on an initially empty substrate or lattice with the restriction that they must not overlap with previously added objects [24–27]. The kinetics of the process is characterized by the time evolution of the coverage, $\theta(t)$, i.e. the fraction of the substrate covered by the deposited objects. This dependence has been the object of numerous analysis, which include Monte Carlo approaches [28–32], series expansion [33, 34], and rate equations [35, 36]. Due to the blocking of the substrate area by the previously adsorbed particles, at large times the coverage $\theta(t)$ approaches the jammed-state value θ_J , where only gaps too small to accommodate new particles are left in the monolayer.

Percolation in RSA systems assumes the existence of a spanning cluster formed by the deposited objects that reaches two opposite sides of the lattice. In such systems, the value of percolation threshold θ_p^* is below the jamming limit θ_J for the deposited shapes. Interplay between jamming density θ_J and percolation threshold θ_p^* has been

Percolation in random sequential adsorption of polydisperse mixtures of extended objects on a triangular lattice studied in detail for a large number of different objects [21, 37–45]. In reference [21] the results for the percolation thresholds, jamming coverages and their ratios were given for the deposition of various shapes on a triangular lattice. It was found that for elongated shapes the percolation threshold monotonically decreases, while for more compact shapes it monotonically increases with the object size. For various objects of the same length, the percolation threshold of more compact objects exceeds the percolation threshold of the elongated ones.

Polydispersity of incident particle size is observed in a large number of processes, especially in colloidal particle and macromolecule adsorption. Irreversible deposition in polydisperse systems was studied for binary mixtures [46–50], and for mixtures of particles obeying various size distributions [51–55]. The impact upon the percolation threshold of accounting for polydispersity in the shapes and sizes of the particles has also been examined [56–59]. Efforts that address such non-monodisperse systems are especially relevant in view of the fact that distributions over particle dimensions are often present in experimental situations [60–63]. However, not much is known about the influence of the particle size distribution on the properties of composite materials and there are still many questions to be answered.

In this paper, the percolation behavior of an adsorbed polydisperse mixture has been investigated by using Monte Carlo (MC) simulation and finite-size scaling analysis. Basic depositing shapes, such as k -mers, angled objects, triangles, rhombuses, and hexagons, are made by directed self-avoiding lattice steps [31]. The polydisperse mixtures are made of n objects of various sizes of the same shape. The objects of larger size are made using the same procedure as for the basic ones, with the edges of the shape gradually enlarging the necessary number of times. Simulations are performed for polydisperse mixtures containing isomorphic objects of various sizes which are generated from a specific basic shape. This study examines the influence of the shape of the primary object defining a polydisperse mixture on its percolation and jamming properties. Dependence of the percolation threshold on the number of components making the mixture is also analyzed. Special attention is devoted to the analysis of substrate coverage by individual components forming a mixture at the mixture percolation threshold.

We organized the paper as follows. Section 2 describes the details of the model and simulations. In section 3 results of numerical simulation are presented and discussed. Finally, section 4 contains some additional comments and final remarks.

2. Definition of the model and the simulation method

Depositing objects used in our simulations are made by directed self-avoiding random walks on a triangular lattice. Various shapes of length $\ell = 1, 2,$ and $3,$ and one object of length six with different percolation and jamming behavior, are shown in table 1. A random walk chain of length ℓ covers $k = \ell + 1$ lattice sites. Objects of larger sizes are made by repeating each step of the basic shape the same number of times. In this manner, all objects of larger sizes are isomorphic to the basic shape. In the case of compact basic shapes such as triangles, rhombuses and hexagons, larger objects also occupy all comprised sites. Formation of objects larger than the basic ones is illustrated in table 2. The polydisperse mixtures are made of n objects of sequentially increasing

Table 1. Basic objects of various shapes. The number of nearest neighbors is denoted by $m^{(x)}$ for the corresponding shape, and ℓ denotes the length of the walk that makes the shape.
























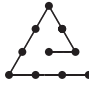


(x)	Shape	$m^{(x)}$	$\ell^{(x)}$
(A)		8	1
(B)		10	
(C)		10	2
(D)		9	
(E)		12	
(F)		12	
(G)		11	
(H)		12	3
(I)		12	
(J)		10	
(K)		12	6

Table 2. Illustration of the construction of the objects larger than the basic ones.

k -mer	ℓ	Angle (C)	ℓ	Triangle	ℓ	Rhombus	ℓ	Hexagon	ℓ
	1		2		2		3		6
	2		4		5		8		18
	3		6		9		15		36
...

sizes of the basic shape, or of n objects of various shapes of the same length. Size of the object is determined by the length ℓ of the walk making the object.

Monte Carlo simulations are performed on a triangular lattice with linear size up to $L = 3200$ sites. At each Monte Carlo step a lattice site is selected at random. If the selected site is unoccupied, one of the objects making the mixture is chosen with equal probability and deposition of the selected object is tried in one of the six orientations. We fix the beginning of the walk that makes the shape at the selected site, and search whether all successive ℓ sites are unoccupied. If so, we occupy these $\ell + 1$ sites and deposit the object. If the attempt fails, deposition of a new object from the mixture is tried at a new randomly chosen site.

During the process, the coverage of the surface is increased, and the percolation threshold θ_p is reached when a cluster that extends through the whole system appears. Here we check the connectivity between the left and the right edges of the lattice. The tree-based union/find algorithm is used to determine the percolation threshold [64]. Each cluster of connected sites is stored as a separate tree, having a single ‘root’ site. All sites in the cluster possess pointers to the root site, making it simple to ascertain whether two sites belong to the same cluster. When a deposited object connects two separated clusters, they are amalgamated by adding a pointer from the root of the smaller cluster to the root of the larger one. This procedure is repeated until the percolation threshold is reached, i.e. until the opposite sides of the lattice are connected by a single cluster.

Another quantity of interest is the jamming limit θ_j when neither of the shapes making the mixture can be placed in any position on the lattice. The jamming limit is reached when the number of inaccessible sites (the occupied sites and the sites that cannot be the beginning of any walk making the mixture) becomes equal to the total number of lattice sites L^2 . For the approach to the jamming coverage and percolation, periodic boundary conditions are used in all directions. The time is counted by the number of attempts to select a lattice site and scaled by the total number of lattice sites. The data is averaged over 500 independent runs for each mixture of depositing objects, and each lattice size L .

3. Results and discussion

Simulations are performed for n -component mixtures of objects of various sizes, where all objects in the mixture are isomorphic to a single basic object from table 1. The number of components n is always increased by adding an object of a greater length, starting from the basic one. For example, the two-component mixture of line segments consists of the lines of length $\ell = 1$ and $\ell = 2$, the three-component mixture is made by adding a line segment of length $\ell = 3$, and so on. An n -component mixture contains lines of length $\ell = 1, 2, \dots, n$, and all of them are adsorbed with equal probability. Mixtures of the other shapes from table 1 are made in a similar way. In the case of k -mers, mixture with up to $n = 30$ components are examined, mixtures of angled objects are made up to $n = 10$, and mixtures of triangles, as well as the other basic objects from table 1, contain up to $n = 5$ components.

For percolation-type systems, it is known that the dependence of the effective percolation threshold θ_p (the mean value of threshold measured for a finite lattice) on the linear size L of the lattice is described by the finite-size scaling theory [3]. The effective percolation threshold θ_p approaches the asymptotic value θ_p^* for $L \rightarrow \infty$ via the power law:

$$\theta_p - \theta_p^* \propto L^{-1/\nu}. \quad (1)$$

Here θ_p^* is the exact percolation threshold (as $L \rightarrow \infty$), and ν is the correlation length critical exponent. For two-dimensional systems the theoretical value for correlation length is $\nu = 4/3$. Relationship (1) allows us to extrapolate the percolation threshold for an infinite system.

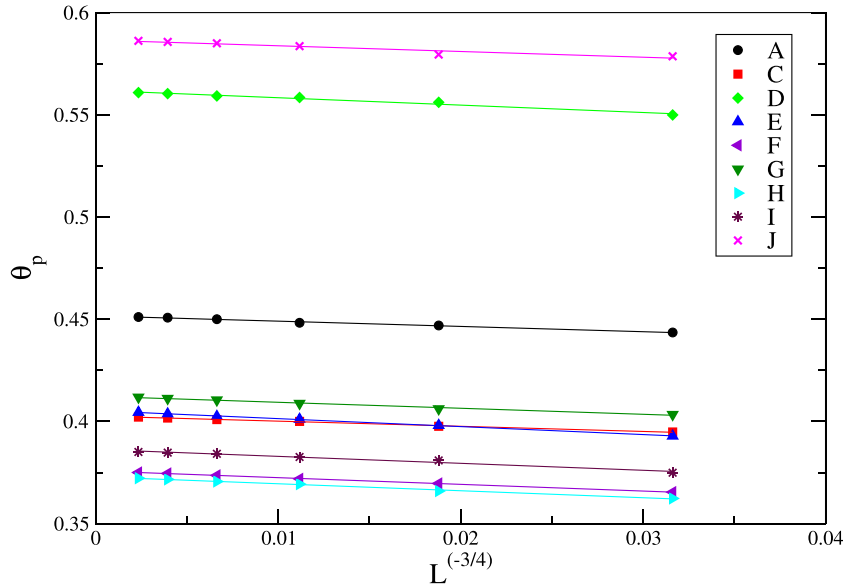


Figure 1. Finite-size scaling of the percolation threshold θ_p against $L^{-1/\nu}$, with $\nu = 4/3$, for the four-component mixtures of the basic objects shown in the legend (see, table 1). Each mixture is made of four different sizes of the basic shape.

Simulations were performed for lattice sizes ranging from $L = 100$ to $L = 3200$. Plotting the obtained values of the effective percolation threshold θ_p for various lattice sizes against $L^{-1/\nu}$ confirms the validity of the finite-size scaling in the system and determines the asymptotic value of the percolation threshold θ_p^* . In figure 1 finite-size scaling of the percolation threshold θ_p is illustrated for the four-component mixtures of the basic shapes shown in table 1. Each mixture contains objects (components) of four sizes that correspond to a specific basic shape.

Dependence of the percolation threshold θ_p^* on the number of mixture components n is shown in figure 2 for various basic shapes from table 1. For comparison, results are shown for mixtures containing $n = 1, 2, \dots, 5$ components. The exceptions are made for rhombuses (J) and hexagons (K). Namely, maximum number of mixture components that exhibit percolation is $n = 4$ for rhombuses, and $n = 3$ for hexagons. From this figure it can be seen that for the elongated objects, such as k -mers (A), angled objects (C), objects (F), (G), (H), and (I) from table 1, percolation threshold θ_p^* decreases with the number of mixture components. For these shapes percolation is reached more easily with adding a longer component to the mixture. During deposition, larger objects form large compact clusters of parallel objects. By effectively connecting, they create a porous deposit, which reduces the percolation threshold. On the contrary, compact and larger objects, such as triangles (D), rhombuses (J), and hexagons (K), are significantly more difficult to connect into large clusters. During deposition, they effectively fill the surface with groups of smaller and disconnected clusters, which increases the percolation threshold θ_p^* with the number of components.

Percolation properties depend on the connectivity of depositing shapes, i.e. on the capability of the object to make connections with other depositing objects. The number of nearest neighbors m seems to be a quantity that is closely related to the connectivity,

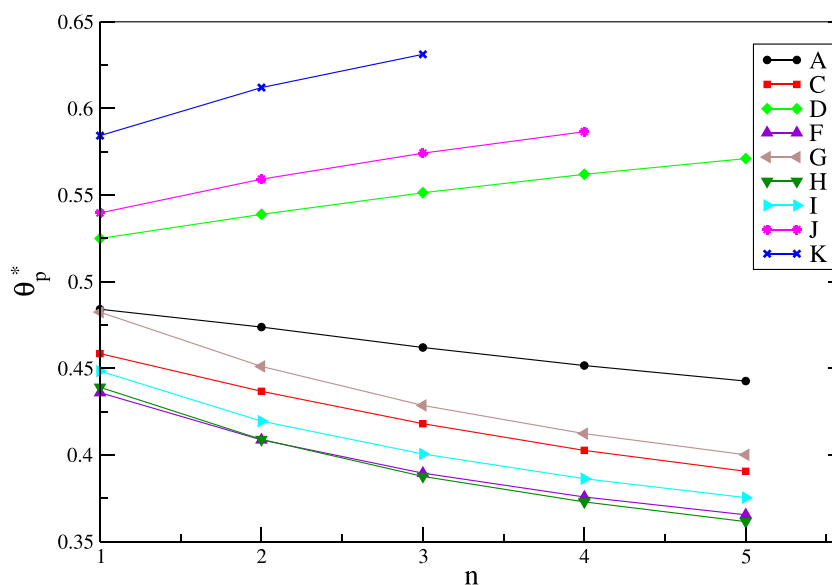


Figure 2. Dependence of the percolation threshold θ_p^* on the number of mixture components n for various basic shapes given in the legend (see, table 1). The number of components n is always increased by adding an object of a greater length.

Table 3. Values of the percolation thresholds θ_p^* for various number of mixture components n . Basic shapes are denoted as in table 1.

n	1	2	3	4	5
(A)	0.4841(13)	0.4738(2)	0.4620(1)	0.4516(2)	0.4427(2)
(C)	0.4585(11)	0.4367(1)	0.4180(2)	0.4026(2)	0.3906(3)
(D)	0.5249(1)	0.5389(1)	0.5513(3)	0.5620(5)	0.5710(4)
(F)	0.4360(2)	0.4087(2)	0.3895(2)	0.3758(1)	0.3655(2)
(G)	0.4824(2)	0.4511(2)	0.4286(2)	0.4123(3)	0.4001(1)
(H)	0.4391(1)	0.4090(1)	0.3876(2)	0.3729(2)	0.3615(2)
(I)	0.4484(3)	0.4195(1)	0.4006(3)	0.3863(5)	0.3754(5)
(J)	0.5397(4)	0.5592(2)	0.5742(2)	0.5866(7)	
(K)	0.5843(2)	0.6120(4)	0.6312(2)		

and it is included in table 1. It was shown that the percolation threshold decreases with m for objects of the same length [21]. This feature reflexes also in the case of deposition of mixtures of objects of various sizes of the same basic shape. For mixtures of elongated objects, having larger number of nearest neighbours, the percolation threshold decreases with adding longer objects to the mixtures. On the other hand, for mixtures of compact objects (triangles, rhombuses and hexagons) the percolation threshold increases with the number of components and the percolation can be reached only for a relatively low number of mixture components. Values of the percolation thresholds θ_p^* are given in table 3 for $n = 1, 2, \dots, 5$ component mixtures. Results are presented for all different basic objects of length $\ell = 1, 2$ and 3.

Comparison of the percolation properties of n -component mixtures and of the single objects of various sizes ($\ell \leq n$) is given in figure 3. Dependence of the percolation threshold θ_p^* on the number of components n making the mixture is shown with filled symbols and solid lines, and the dependence on the length ℓ of the single mixture components with open symbols and dashed lines. Results for objects (B), (C), and (D) are shown in figure 3(a). The percolation threshold of mixture of k -mers monotonically decreases with the number n of k -mers making the mixture, i.e. with the longest mixture component. On the other hand, the percolation threshold of single k -mers decreases with the k -mer length, reaches a minimum, and increases for longer k -mers. For large enough number of mixture components n , lower values of the percolation threshold can be reached in the case of mixtures than in the case of single k -mers of the corresponding the largest component length. Percolation threshold θ_p^* for the angled objects also decreases with the number of mixture components, but the decrease of θ_p^* is even sharper with the growth of the single angled objects. Adding larger triangles to the mixtures leads to higher values of the percolation threshold, while the percolation threshold θ_p^* grows faster with the single objects size. The connectivity in the system is very poor for large compact objects, but it is enhanced by the presence of smaller objects.

From figures 3(b) and (c) we can see that the percolation threshold monotonically decreases with n for the elongated shapes (F), (G), (H), and (I). Mixtures of the elongated shape (H) give the onset of percolation approximately at the same coverages as the largest mixture components. For the less elongated shapes (G) and (I) the percolation threshold for mixtures is higher than for the largest objects making the mixture. For rhombuses (J), as compact objects, value of the percolation threshold increases with the number of mixture components, as well as with the single object size determined with the length ℓ of the walk.

Figure 4 presents the partial percolation coverages of all components at percolation thresholds θ_p^* for mixtures of k -mers, angled objects, and triangles. The partial percolation thresholds represent the contribution of individual components in the lattice covering at the percolation threshold for n -component mixture. For the two-component mixture of k -mers, the fractional participation of dimers in the percolation threshold is 0.46, and 0.54 for three-mers. In mixtures with a sufficiently large number of components, the contribution of large components in percolation coverages decreases as their size increases. Similar results obtained for the mixtures of the basic components covering four lattice sites, (F), (G), (H), (I), and (J), are shown in figure 5.

Comparison of the percolation threshold θ_p^* and the jamming coverage θ_J on the number of components n for polydisperse mixtures of k -mers, angled objects, and triangles is given in figure 6. For mixtures of k -mers, the jamming coverage θ_J slightly grows with n , while for the angled objects slightly decreases. For compact triangles jamming value θ_J , as well as the percolation threshold θ_p^* , grows with adding larger objects to the mixture. Jamming coverages θ_J of polydisperse mixtures that correspond to the basic objects (E), (F), (G), (H), (I), and (J) are shown in figure 7. The only object that exhibits the decrease of the jamming coverage with adding larger objects to the mixture is object (H), while the sharpest increase is for the mixtures of rhombuses (J). On the other hand, the percolation threshold θ_p^* decreases for most of these mixtures, as can be seen from figure 2, and increases for the rhombuses.

Percolation in random sequential adsorption of polydisperse mixtures of extended objects on a triangular lattice

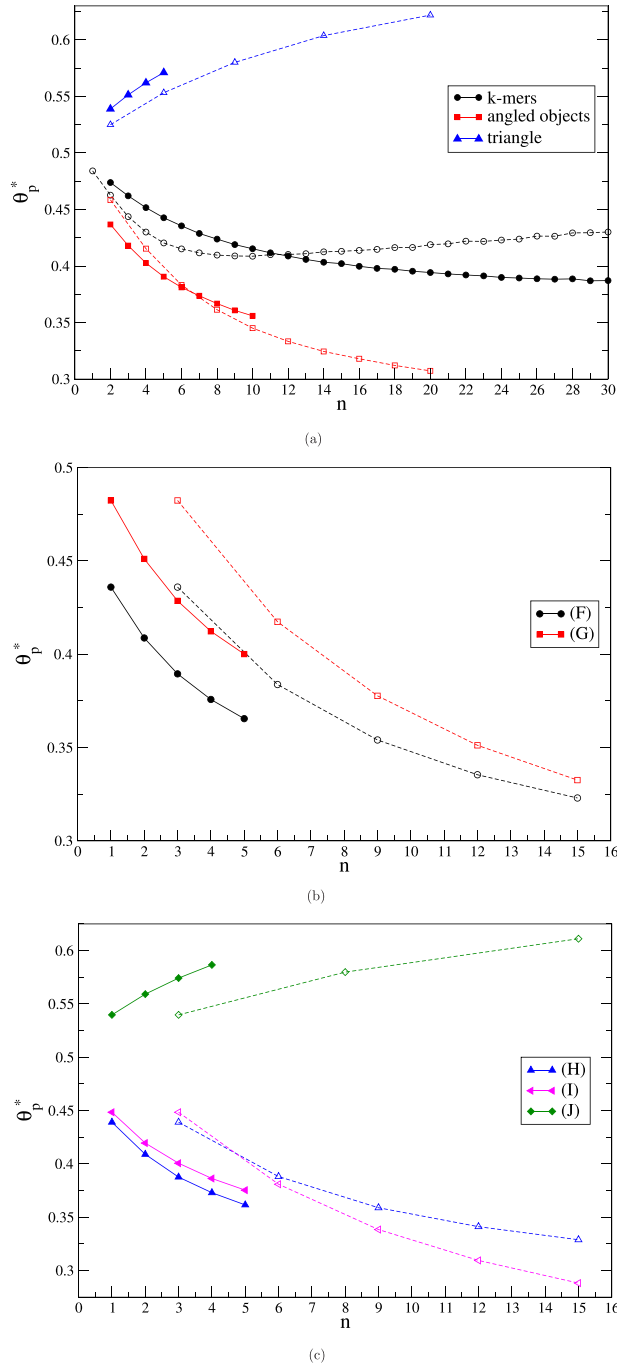


Figure 3. Dependence of the percolation threshold θ_p^* on the number n of components making the mixture (filled symbols and solid lines) and on the length ℓ of the single mixture components (open symbols and dashed lines) for: (a) k -mers, angled objects, and triangles; (b) basic shapes (F), and (G); (c) basic shapes (H), (I), and (J) (see, table 1). The number of components n is always increased by adding an object of a greater length.

Percolation in random sequential adsorption of polydisperse mixtures of extended objects on a triangular lattice

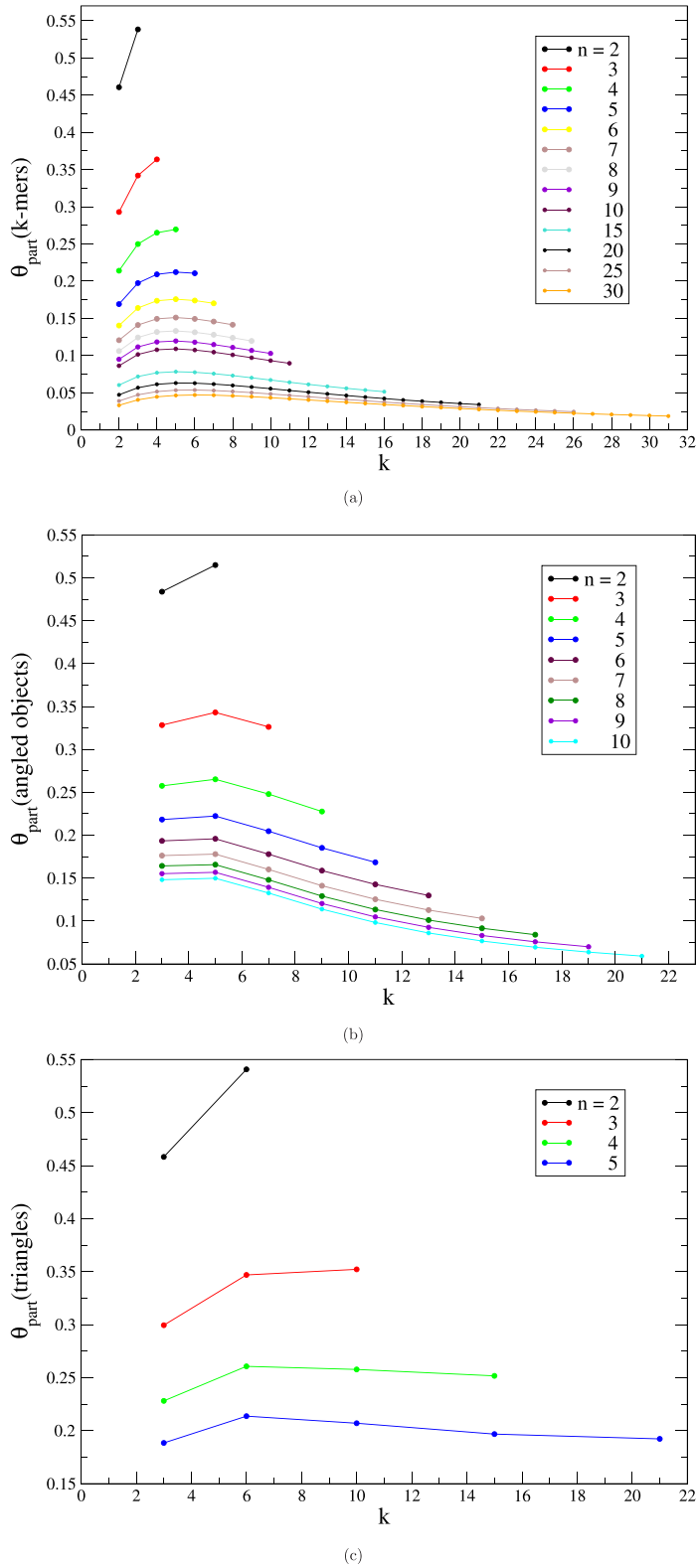


Figure 4. The partial percolation coverages *vs* the number of sites $k = \ell + 1$ covered by the component shapes for n -component mixtures of (a) k -mers, (b) angled objects, and (c) triangles.

Percolation in random sequential adsorption of polydisperse mixtures of extended objects on a triangular lattice

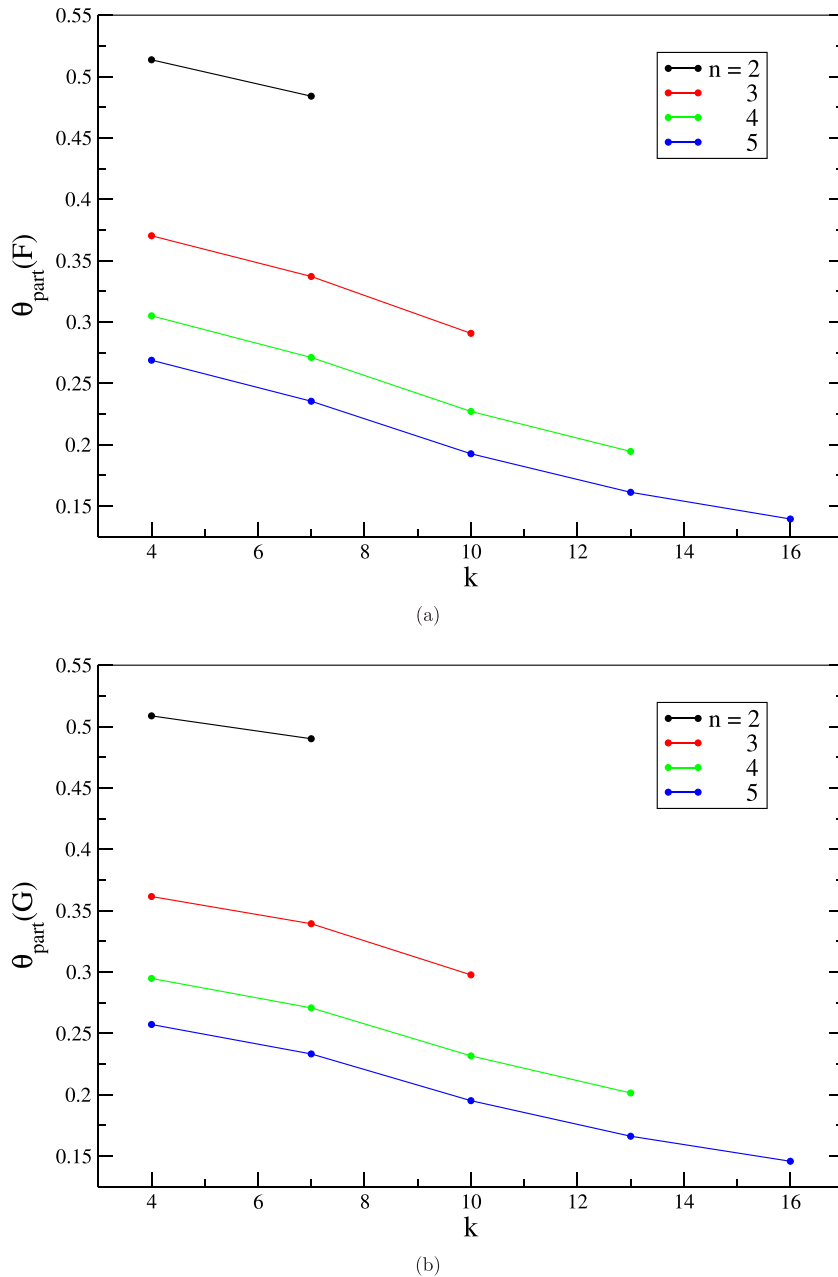
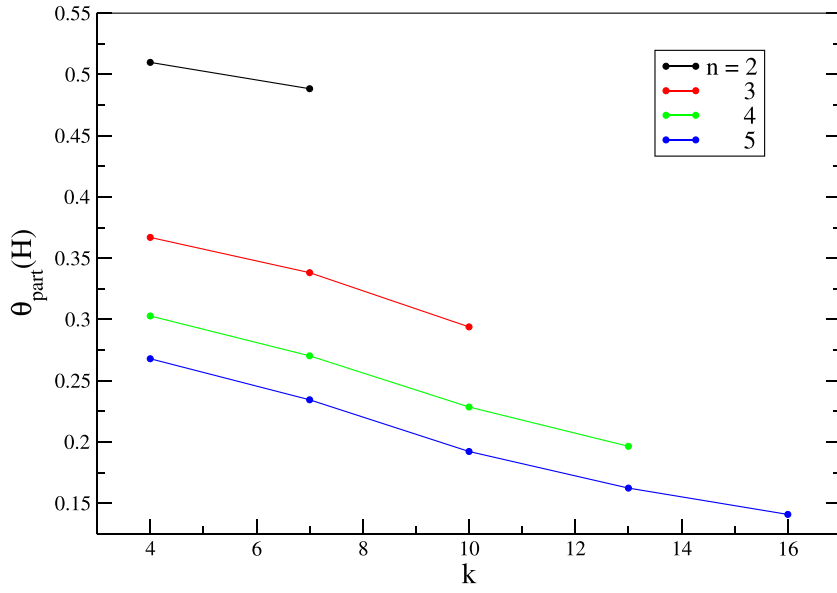


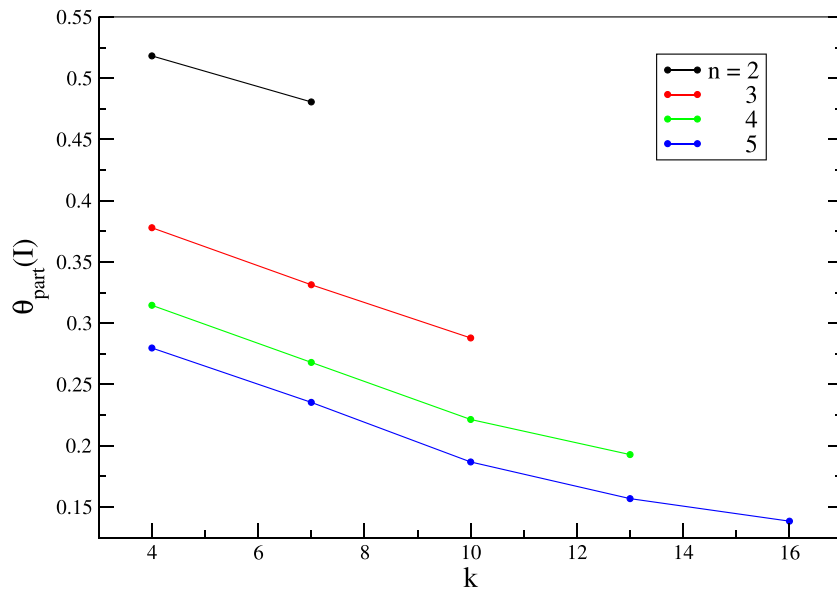
Figure 5. The partial percolation coverages *vs* the number of sites $k = \ell + 1$ covered by the component shapes for n -component mixtures of objects (a) (F), (b) (G), (c) (H), (d) (I), and (e) (J) (see, table 1).

The obtained results can be more easily intuitively understood through visual observation of the coverage achieved for various object combinations. Some typical snapshot configurations at the percolation threshold are shown in figure 8. The snapshots of size $\Delta L^2 = 100^2$ are taken from the central part of the lattice. Five-component mixtures of angled objects (C), (H), and (J) give porous configurations thanks to their good connectivity, leading to low values of the percolation thresholds. On the other hand,

Percolation in random sequential adsorption of polydisperse mixtures of extended objects on a triangular lattice



(c)



(d)

Figure 5. (Continued.)

mixtures of compact objects, such as triangles and rhombuses, cover the surface more efficiently, at the same time having a lower connecting probability. This results in higher values of the percolation threshold, while for mixtures with larger number of components percolation cannot be reached. For triangles, maximum number of components that exhibits percolation transition is five, for rhombuses four, and for hexagons three.

Mixtures of objects of the same size and various shapes are studied for objects of sizes $\ell = 2$ and 3. The percolation properties of a three-component mixture of linear

Percolation in random sequential adsorption of polydisperse mixtures of extended objects on a triangular lattice

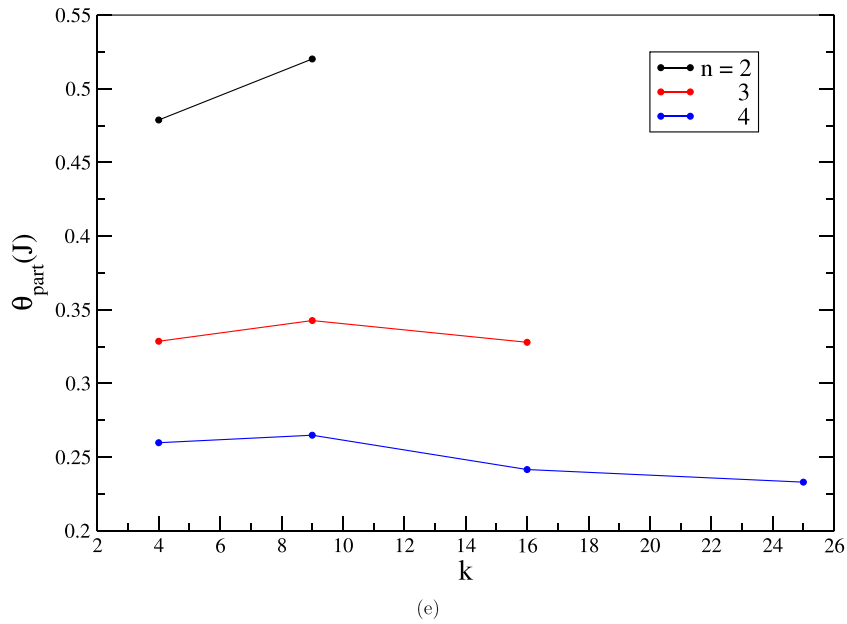


Figure 5. (Continued.)

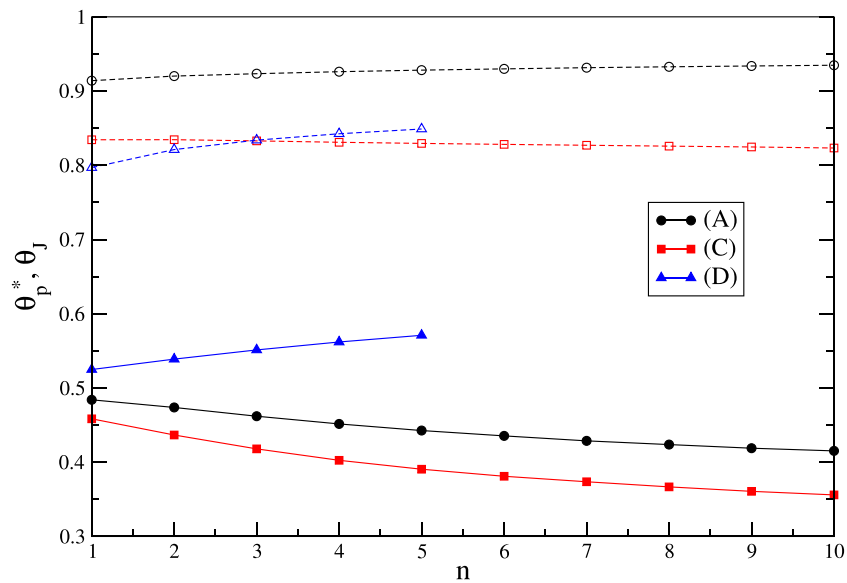


Figure 6. Comparison of the percolation coverage θ_p^* (filled circles and solid lines) and the jamming coverage θ_J (open symbols and dashed lines) on the number of mixture components n of k -mers, angled objects, and triangles. The number of components n is always increased by adding an object of a greater length.

objects, angled shapes, and triangles are analyzed. In addition, various multi-component mixtures of objects of size $\ell = 3$ are also studied. Results for the percolation thresholds θ_p^* for these mixtures are given in table 4. It is interesting to note that the values of the

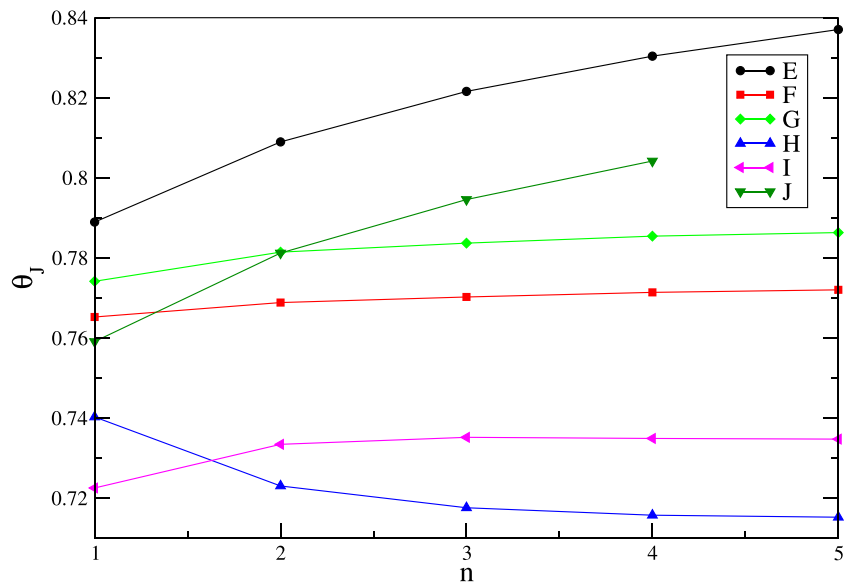
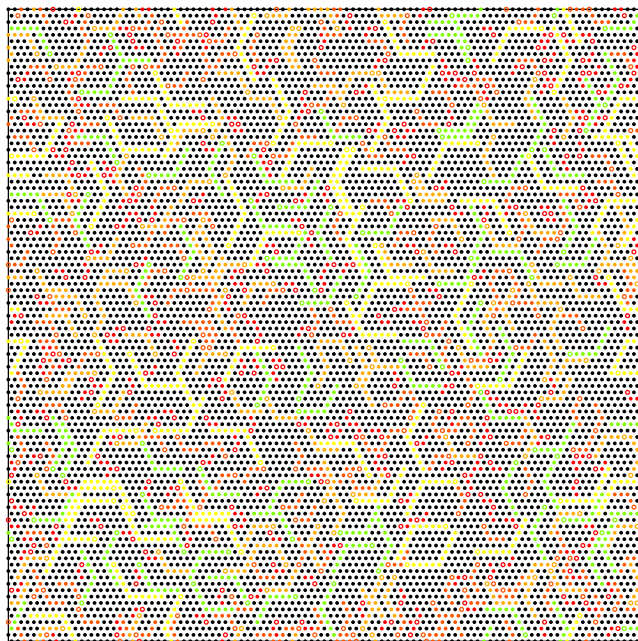
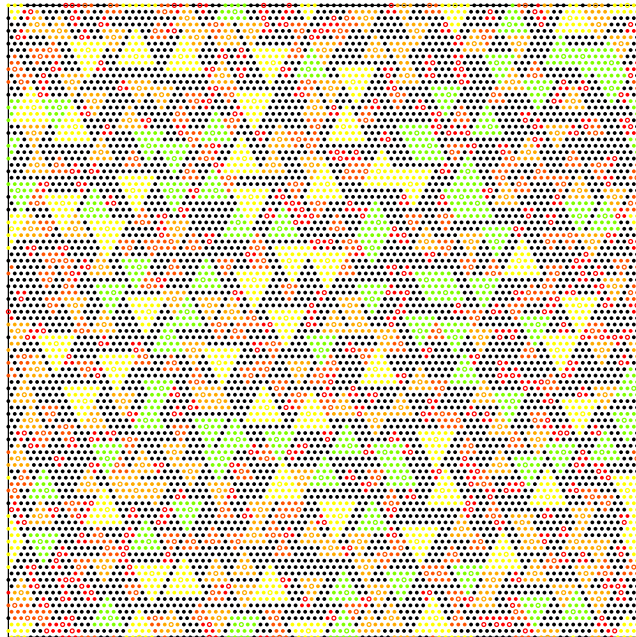


Figure 7. Dependence of the jamming coverage θ_J of polydisperse mixture on the number of components n for the basic shapes given in the legend (see, table 1).

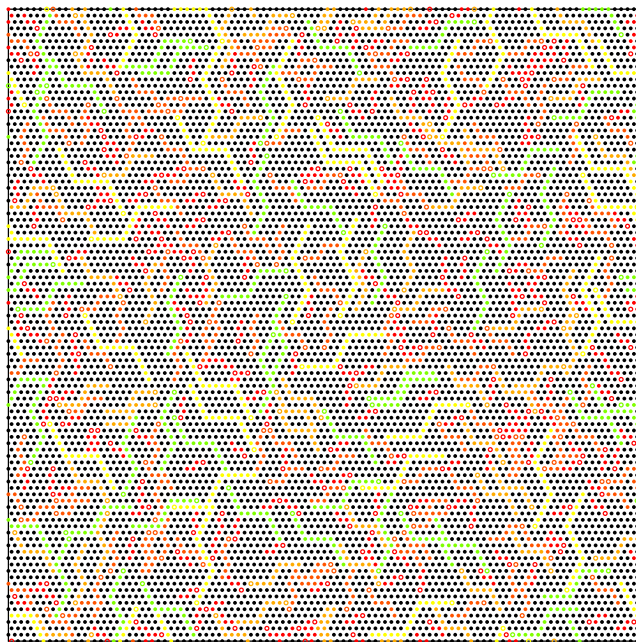


(a)

Figure 8. Typical configurations for five-component mixtures of basic shapes: (a) angled objects (C), (b) triangles (D), (c) (H), (d) (I), (e), and for a four-component mixture of rhombuses (J) at the percolation thresholds θ_p^* (see, table 1). The snapshots were made at the moment of percolation cluster formation. Objects of different sizes are distinguished by color. Empty lattice nodes are black. Open circles represent the ‘heads’ of objects (the starting point of a random walk).



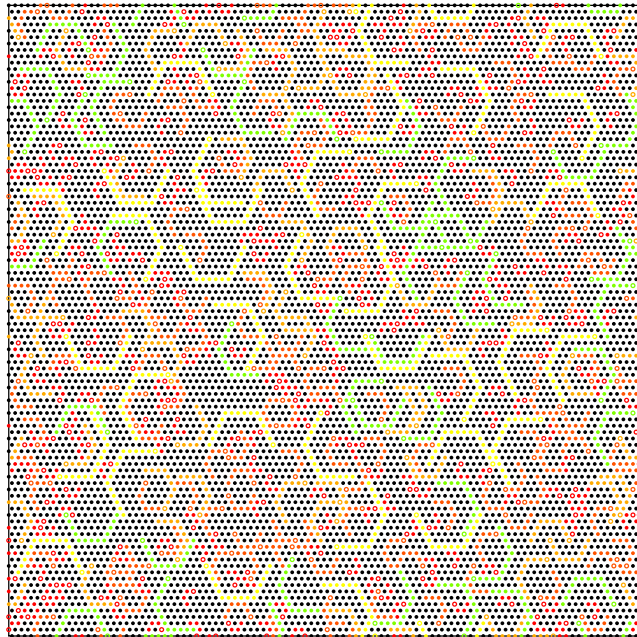
(b)



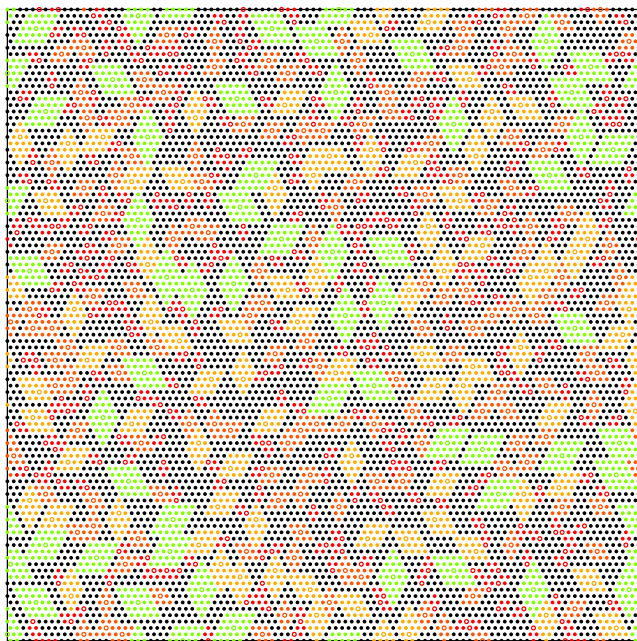
(c)

Figure 8. (Continued.)

percolation threshold θ_p^* (mixture) for these mixtures are very close to the mean values for θ_p^* of the corresponding components. For the three-component mixture of objects (B), (C) and (D) this difference is on the fourth given digit, while for various mixtures of length $\ell = 3$, the difference can be noticed at the third given digit. This leads to the



(d)



(e)

Figure 8. (Continued.)

conclusion that a certain value of the percolation threshold can be obtained by choosing the right concentration of mixture components. Also, the percolation thresholds can be tuned by adding objects of various sizes to the mixtures.

Table 4. Values of the percolation thresholds $\theta_p^{*(x)}$ for single objects (x) and mixtures $\theta_p^*(\text{mixt.})$. The numbers in parentheses are the numerical values of the standard uncertainty of $\theta_p^{*(x)}$ and $\theta_p^*(\text{mixt.})$ referred to the last digits of the quoted value.

(x)	ℓ	$\theta_p^{*(x)}$	Mixture	$\theta_p^*(\text{mixt.})$
(B)	2	0.4611 (9)	(B)+(C)+(D)	0.48 066 (16)
(C)		0.4585 (11)		
(D)		0.5214 (9)		
(E)	3	0.4399 (12)	(G)+(J)	0.51 121 (11)
(F)		0.4304 (12)	(E)+(H)+(J)	0.46 591 (11)
(G)		0.4815 (11)	(E)+(F)+(G)+(H)+(I)+(J)	0.46 148 (10)
(H)		0.4369 (11)	(F)+(G)+(I)	0.45 516 (17)
(I)		0.4461 (5)	(E)+(F)+(H)+(I)	0.43 747 (10)
(J)		0.5387 (6)		

4. Concluding remarks

Percolation phenomena have been investigated in irreversible deposits of polydisperse mixtures. Depositing objects of various sizes and shapes were made by directed self-avoiding walks on the triangular lattice. Special attention has been paid to deposition of mixtures containing objects of the same shape, but various sizes. Objects of larger sizes were made by repeating each step of the basic shape the same number of times. In the case of compact objects, such as triangles, rhombuses and hexagons—larger objects of these basic shapes also occupied all comprised sites. For all possible basic shapes covering $k = 2, 3$ and 4 lattice sites, n -component mixtures were made. The number of mixture components n was always increased by adding a larger object.

It was found that for elongated objects the percolation threshold θ_p^* decreased with the number of components, i.e. with adding larger objects to the mixture. This was the case especially for the objects that have greater possibilities for blocking of comprised sites, such as angled objects. Objects of this type make more porous deposits, and the porosity is more pronounced with adding larger objects to the mixtures. On the contrary, for compact objects, such as triangles, rhombuses and hexagons, percolation threshold increased with n , and the percolation could be reached only for relatively low number of these compact mixture components.

Percolation properties depend on the connectivity of depositing shapes, that is related to the number of nearest neighbors m , for the one-component deposits, as well as for the mixtures. Larger m makes formation of the paths through the deposit easier, and the percolation sets on at lower coverages.

Mixtures of objects of the same size, but of various shapes, were also investigated. It was found that the values of the percolation threshold for these mixtures were very close to the mean values of θ_p^* of the corresponding components. Adding objects of various sizes to the mixtures has a greater influence on the percolation threshold than the shape of mixture components.

Acknowledgments

This work was supported by the Ministry of Education, Science and Technological Development of the Republic of Serbia. Numerical simulations were run on the PARADOX supercomputing facility at the Scientific Computing Laboratory of the Institute of Physics Belgrade.

References

- [1] Broadbent S R and Hammersley J M 1957 Percolation processes: I. Crystals and mazes *Math. Proc. Camb. Phil. Soc.* **53** 629–41
- [2] Essam J W 1980 Percolation theory *Rep. Prog. Phys.* **43** 833
- [3] Aharony A and Stauffer D 2003 *Introduction to Percolation Theory* revised 2nd edn (Taylor & Francis)
- [4] Grimmett G 1999 What is percolation? *Percolation* (Springer) pp 1–31
- [5] Sahimi M 2023 *Applications of Percolation Theory (Applied Mathematical Sciences)* 2nd edn (Springer International Publishing)
- [6] Sahimi M and Hunt A G (eds) 2021 *Complex Media and Percolation Theory (Encyclopedia of Complexity and Systems Science Series)* (Springer)
- [7] Hunt A, Ewing R and Ghanbarian B 2014 *Percolation Theory for Flow in Porous Media (Lecture Notes in Physics)* 3rd edn (Springer)
- [8] Cametti C, Codastefano P, Tartaglia P, Rouch J and Chen S H 1990 Theory and experiment of electrical conductivity and percolation locus in water-in-oil microemulsions *Phys. Rev. Lett.* **64** 1461
- [9] Octavio M, Octavio A, Aponte J, Medina R and Lobb C J 1988 Nonuniversal critical behavior in the critical current of superconducting composites *Phys. Rev. B* **37** 9292
- [10] Heyes D M and Melrose J R 1988 Percolation thresholds of simple fluids *J. Phys. A: Math. Gen.* **21** 4075
- [11] Chatterjee A P 2000 Continuum percolation in macromolecular fluids *J. Chem. Phys.* **113** 9310
- [12] Dalmas F, Dendievel R, Chazeau L, Cavallé J-Y and Gauthier C 2006 Carbon nanotube-filled polymer composites. Numerical simulation of electrical conductivity in three-dimensional entangled fibrous networks *Acta Mater.* **54** 2923
- [13] Foygel M, Morris R D, Anez D, French S and Sobolev V L 2005 Theoretical and computational studies of carbon nanotube composites and suspensions: electrical and thermal conductivity *Phys. Rev. B* **71** 104201
- [14] Song Y, Lee S-I and Gaines J R 1992 AC conduction and 1/f noise in a Cr-film lattice-percolation system *Phys. Rev. B* **46** 14
- [15] Day A, McGurn A, Bergman D and Thorpe M 2003 Spectral representation of the electrical properties of layered materials, *Physica B* **338** 24
- [16] Sokółowska D, Król-Otwinowska A and Mościcki J K 2004 Water-network percolation transitions in hydrated yeast *Phys. Rev. E* **70** 052901
- [17] Re A, Cora D, Puliti A M, Caselle M and Sbrana I 2006 Correlated fragile site expression allows the identification of candidate fragile genes involved in immunity and associated with carcinogenesis *BMC Bioinform.* **7** 413
- [18] Lebrecht W, Centres P and Ramirez-Pastor A 2019 Analytical approximation of the site percolation thresholds for monomers and dimers on two-dimensional lattices *Physica A* **516** 133
- [19] Kondrat G 2008 Impact of composition of extended objects on percolation on a lattice *Phys. Rev. E* **78** 011101
- [20] Cornette V, Ramirez-Pastor A and Nieto F 2003 Dependence of the percolation threshold on the size of the percolating species *Physica A* **327** 71
- [21] Budinski-Petković L, Lončarević I, Petković M, Jakšić Z M and Vrhovac S B 2012 Percolation in random sequential adsorption of extended objects on a triangular lattice *Phys. Rev. E* **85** 061117
- [22] Dujak D, Karač A, Budinski-Petković L, Lončarević I, Jakšić Z M and Vrhovac S B 2019 Percolation in random sequential adsorption of mixtures on a triangular lattice *J. Stat. Mech.* **113210**
- [23] Lončarević I, Budinski-Petković L, Dujak D, Karač A, Jakšić Z M and Vrhovac S B 2020 Percolation in irreversible deposition on a triangular lattice: effects of anisotropy *J. Stat. Mech.* **033211**
- [24] Evans J W 1993 Random and cooperative sequential adsorption *Rev. Mod. Phys.* **65** 1281
- [25] Privman V 2000 Dynamics of nonequilibrium deposition *Colloids Surf. A* **165** 231
- [26] Talbot J, Tarjus G, Van Tassel P and Viot P 2000 From car parking to protein adsorption: an overview of sequential adsorption processes *Colloids Surf. A* **165** 287

- [27] Cadilhe A, Araújo N A M and Privman V 2007 Random sequential adsorption: from continuum to lattice and pre-patterned substrates *J. Phys.: Condens. Matter* **19** 065124
- [28] Nakamura M 1987 Percolational and fractal property of random sequential packing patterns in square cellular structures *Phys. Rev. A* **36** 2384
- [29] Vigil R D and Ziff R M 1990 Kinetics of random sequential adsorption of rectangles and line segments *J. Chem. Phys.* **93** 8270
- [30] Sherwood J D 1990 Random sequential adsorption of lines and ellipses *J. Phys. A: Math. Gen.* **23** 2827
- [31] Sherwood J D 1997 Random sequential adsorption on a triangular lattice *Phys. Rev. E* **56** 6904
- [32] Lončarević I, Budinski-Petković L, Šćepanović J R, Jakšić Z M and Vrhovac S B 2020 Random sequential adsorption of lattice animals on a three-dimensional cubic lattice *Phys. Rev. E* **101** 012119
- [33] Bonnier B, Hontebeyrie M, Leroyer Y, Meyers C and Pommiers E 1994 Adsorption of line segments on a square lattice *Phys. Rev. E* **49** 305
- [34] Baram A and Fixman M 1995 Random sequential adsorption: long time dynamics *J. Chem. Phys.* **103** 1929
- [35] Talbot J, Tarjus G and Schaaf P 1989 Unexpected asymptotic behavior in random sequential adsorption of nonspherical particles *Phys. Rev. A* **40** 4808
- [36] Evans J W and Nord R S 1985 Random dimer filling of lattices: three-dimensional application to free radical recombination kinetics *J. Stat. Phys.* **38** 681
- [37] Cornette V, Ramirez-Pastor A J and Nieto F 2003 Percolation of polyatomic species on a square lattice *Eur. Phys. J. B* **36** 391
- [38] Vandewalle N, Galam S and Kramer M 2000 A new universality for random sequential deposition of needles *Eur. Phys. J. B* **14** 407
- [39] Kondrat G and Pełkalski A 2001 Percolation and jamming in random sequential adsorption of linear segments on a square lattice *Phys. Rev. E* **63** 051108
- [40] Kondrat G, Koza Z and Brzeski P 2017 Jammed systems of oriented needles always percolate on square lattices *Phys. Rev. E* **96** 022154
- [41] Slutskii M G, Barash L Y and Tarasevich Y Y 2018 Percolation and jamming of random sequential adsorption samples of large linear k -mers on a square lattice *Phys. Rev. E* **98** 062130
- [42] Rampf F and Albano E V 2002 Interplay between jamming and percolation upon random sequential adsorption of competing dimers and monomers *Phys. Rev. E* **66** 061106
- [43] Adamczyk P, Romiszowski P and Sikorski A 2008 A simple model of stiff and flexible polymer chain adsorption: the influence of the internal chain architecture *J. Chem. Phys.* **128** 154911
- [44] Kondrat G 2002 Influence of temperature on percolation in a simple model of flexible chains adsorption *J. Chem. Phys.* **117** 6662
- [45] Longone P, Centres P M and Ramirez-Pastor A J 2012 Percolation of aligned rigid rods on two-dimensional square lattices *Phys. Rev. E* **85** 011108
- [46] Meakin P and Jullien R 1992 Random-sequential adsorption of disks of different sizes *Phys. Rev. A* **46** 2029
- [47] Bonnier B, Leroyer Y and Pommiers E 1992 Random sequential adsorption of line segments : universal properties of mixtures in 1, 2 and 3D lattices *J. Phys. I France* **2** 379
- [48] Lončarević I, Budinski-Petković L and Vrhovac S B 2007 Simulation study of random sequential adsorption of mixtures on a triangular lattice *Eur. Phys. J. E* **24** 19
- [49] Subashiev A V and Luryi S 2007 Fluctuations of the partial filling factors in competitive random sequential adsorption from binary mixtures *Phys. Rev. E* **76** 011128
- [50] Dias C S, Araújo N A M and Cadilhe A 2012 Analytical and numerical study of particles with binary adsorption *Phys. Rev. E* **85** 041120
- [51] Brilliantov N V, Andrienko Y A, Krapivsky P L and Kurths J 1996 Fractal formation and ordering in random sequential adsorption *Phys. Rev. Lett.* **76** 4058
- [52] Adamczyk Z, Siwek B, Zembala M and Weroński P 1997 Influence of polydispersity on random sequential adsorption of spherical particles *J. Colloid Interface Sci.* **185** 236
- [53] Budinski-Petković L, Vrhovac S B and Lončarević I 2008 Random sequential adsorption of polydisperse mixtures on discrete substrates *Phys. Rev. E* **78** 061603
- [54] Marques J F, Lima A B, Araújo N A M and Cadilhe A 2012 Effect of particle polydispersity on the irreversible adsorption of fine particles on patterned substrates *Phys. Rev. E* **85** 061122
- [55] Vieira M C, Gomes M and de Lima J 2011 Effect of particle size distribution and dynamics on the performance of two-dimensional packing *Physica A* **390** 3404
- [56] Chatterjee A P 2010 Connectedness percolation in polydisperse rod systems: a modified Bethe lattice approach *J. Chem. Phys.* **132** 224905

Percolation in random sequential adsorption of polydisperse mixtures of extended objects on a triangular lattice

- [57] Chatterjee A P 2011 A remark concerning percolation thresholds in polydisperse systems of finite-diameter rods *J. Stat. Phys.* **146** 244
- [58] Otten R H J and van der Schoot P 2011 Connectivity percolation of polydisperse anisotropic nanofillers *J. Chem. Phys.* **134** 094902
- [59] Ioselevich A S and Kornyshev A A 2002 Approximate symmetry laws for percolation in complex systems: percolation in polydisperse composites *Phys. Rev. E* **65** 021301
- [60] Ounaies Z, Park C, Wise K, Siochi E and Harrison J 2003 Electrical properties of single wall carbon nanotube reinforced polyimide composites *Compos. Sci. Technol.* **63** 1637
- [61] Bauhofer W and Kovacs J Z 2009 A review and analysis of electrical percolation in carbon nanotube polymer composites *Compos. Sci. Technol.* **69** 1486
- [62] Hu L, Hecht D S and Grüner G 2004 Percolation in transparent and conducting carbon nanotube networks *Nano Lett.* **4** 2513
- [63] Tkalya E, Ghislandi M, Otten R, Lotya M, Alekseev A, van der Schoot P, Coleman J, de With G and Koning C 2014 Experimental and theoretical study of the influence of the state of dispersion of graphene on the percolation threshold of conductive graphene/polystyrene nanocomposites *ACS Appl. Mater. Interfaces* **6** 15113
- [64] Newman M E J and Ziff R M 2001 Fast Monte Carlo algorithm for site or bond percolation *Phys. Rev. E* **64** 016706